Supporting Information for

Carbazole modification of Ruthenium Bipyridine–dicarboxylate Oxygen Evolution Molecular Catalyst

Hiroki Otsuka,[a] Atsushi Kobayashi,*[,a] Masaki Yoshida, [a] and Masako Kato [a,b]

[a]Department of Chemistry, Faculty of Science, Hokkaido University, North-10 West-8, Kita-ku, Sapporo 060-0810, Japan

[b]Department of Applied Chemistry for Environment, School of Biological and Environmental Sciences, Kwansei Gakuin University, 2-1 Gakuen, Sanda, Hyogo 669-1337, Japan.

Contents

Figure S1. UV-Vis absorption spectra of **C0**, **C1** and **C2**……3
Figure S2. DPV curves of complexes **C0** and **C0-Br**……3
Figure S3. Cyclic voltammograms of **C0**, **C1**, **C2**, and cbz-py……4
Figure S4. Changes of cyclic voltammograms during potential sweep cycles of **C1** and **C2**……..5
Table S1. MO energies of each complex……..6
Figure S5. Comparison with experimental spectra in dichloromethane/methanol (v/v=9/1) and simulated absorption spectra by TD-DFT calculations of **C0**, **C1** and **C2**. ……..……..7
Table S2. Wavelength, oscillator strength and contributions of major spin-allowed transitions of **C0**……..……8
Figure S6. Schematic molecular orbital diagrams and orbital shapes of **C0** in the ground S_0 state.…9
Table S3. Wavelength, oscillator strength and contributions of major spin-allowed transitions of **C1**……..……10
Figure S7. Schematic molecular orbital diagrams and orbital shapes of **C1** in the ground S_0 state.…11
Table S4. Wavelength, oscillator strength and contributions of major spin-allowed transitions of **C2**……..……12
Figure S8. Schematic molecular orbital diagrams and orbital shapes of **C2** in the ground S_0 state.…13
Figure S9. Chemical OER plot of **C0**, **C1**, and **C2** under [CAN] range from 60 to 120 mM……14
Figure S10. [Cat.] dependence of OER rate……15
Figure S11. MALDI-MS spectra of the extract from the reaction mixture of **C1**……16
Figure S12. Photochemical OER plots of **C2** without $[Ru(bpy)_3]^{2+}$……..……16
Figure S13. Photochemical OER plot of **C0** in the presence of 2 eq. of cbz-H……17
Figure S14. UV-Vis absorption spectra of reaction mixture after 1 h photolysis for **C2**, **C1** and **C0**…17
Figure S15. Photochemical OER plots of **C0**, **C1** and **C2** with Co^{III} oxidant...……18

Figure S16. ^{1}H NMR spectra of **C1** and **C2**……19
Table S5. Crystallographic parameters of **C2**·$2CH_2Cl_2$……..20
Figure S17. ORTEP drawings of. **C2**·$2CH_2Cl_2$…….21

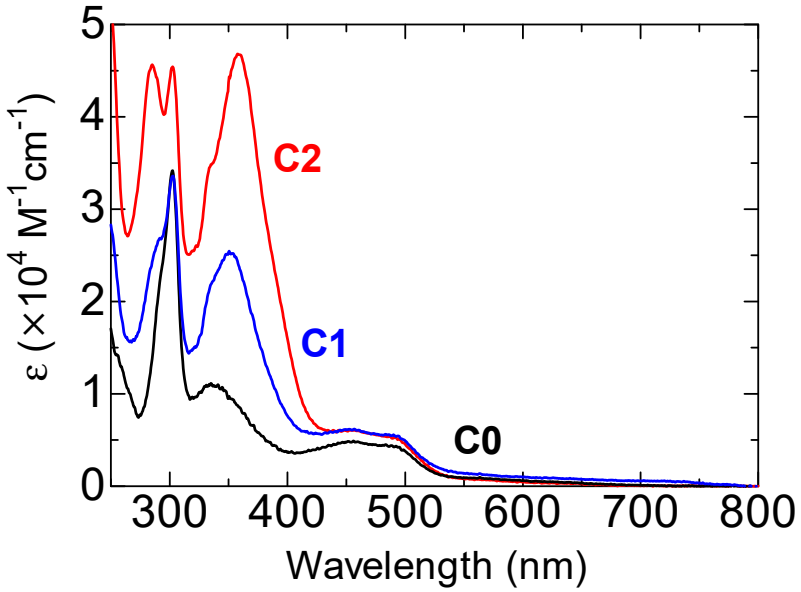

Figure S1. UV-Vis absorption spectra of **C0** (black), **C1** (blue) and **C2** (red). (10 μM, $HClO_4$ aq. (pH = 1.0)/TFE/acetonitrile (v/v/v=3/2/1))

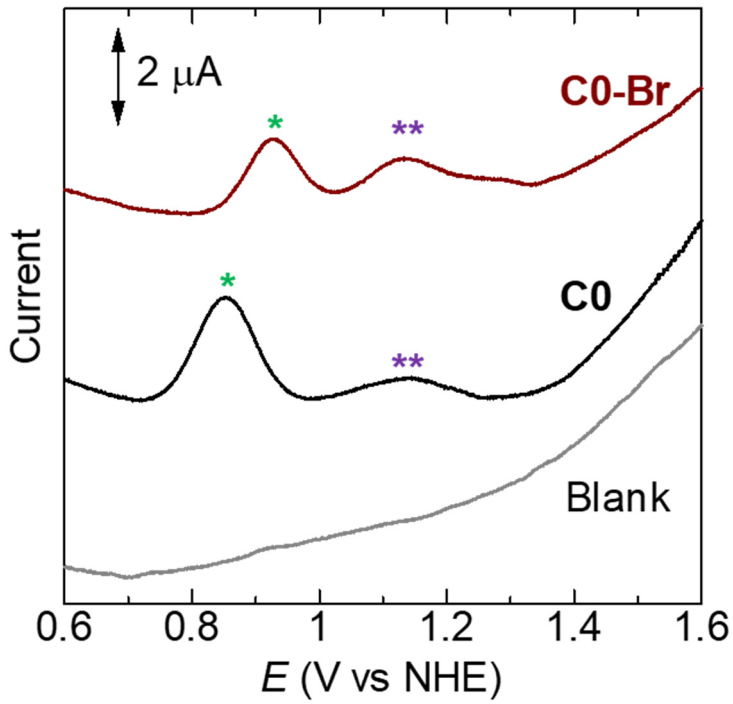

Figure S2. DPV curves of complexes **C0** (black), **C0-Br** (brown) in pH = 1.0 $HClO_4$ aq. /2,2,2-trifluoroethanol(TFE)/ acetonitrile (v/v/v = 3/2/1) containing 0.1 M $NaClO_4$. Scan rate: 10 mVs^{-1}. * and ** are denoted as a redox peak of $Ru^{III/II}$ and $Ru^{IV/III}$, respectively.

(a)

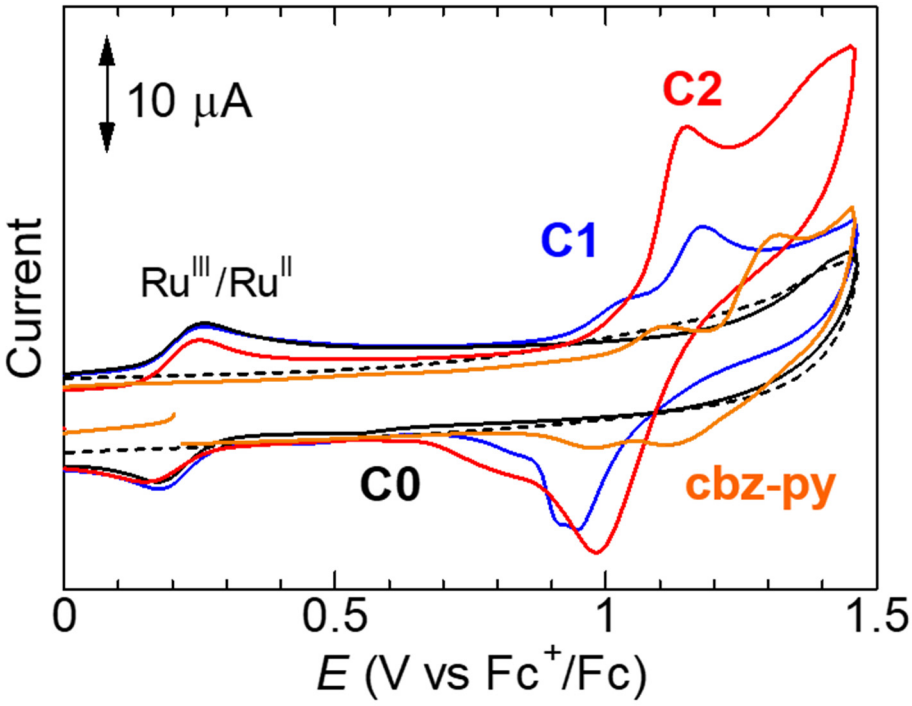

(b)

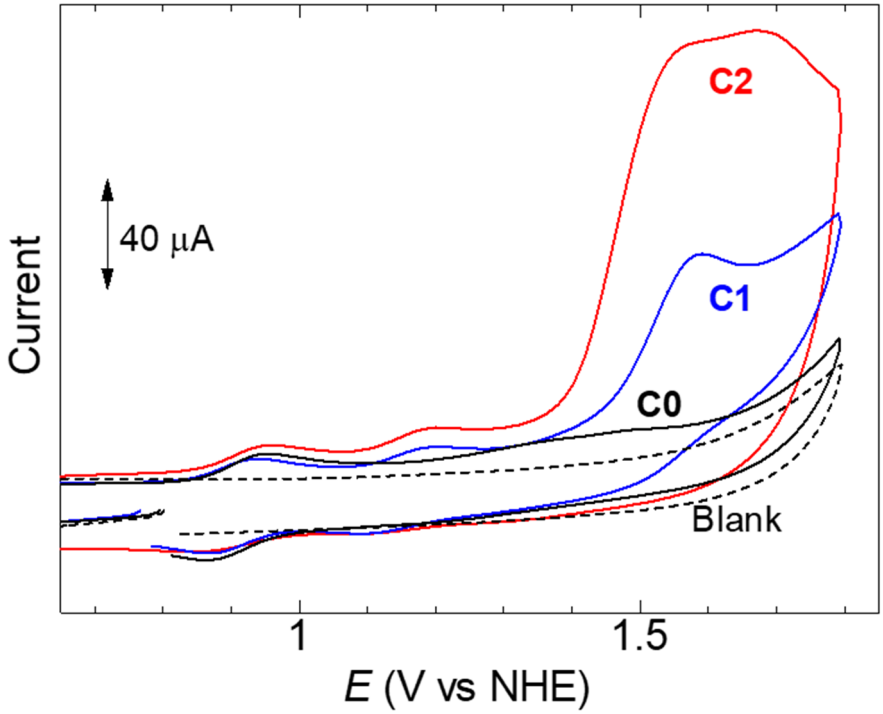

Figure S3. Cyclic voltammograms of **C0**, **C1**, **C2**, and cbz-py in (a) dichloromethane/TFE(v/v=9/1) (200 μM, scan rate 100 mVs^{-1}) and (b) $HClO_4$ aq. (pH = 1.0)/TFE/acetonitrile (v/v/v=1/2/1) (200 μM, scan rate 100 mVs^{-1}).

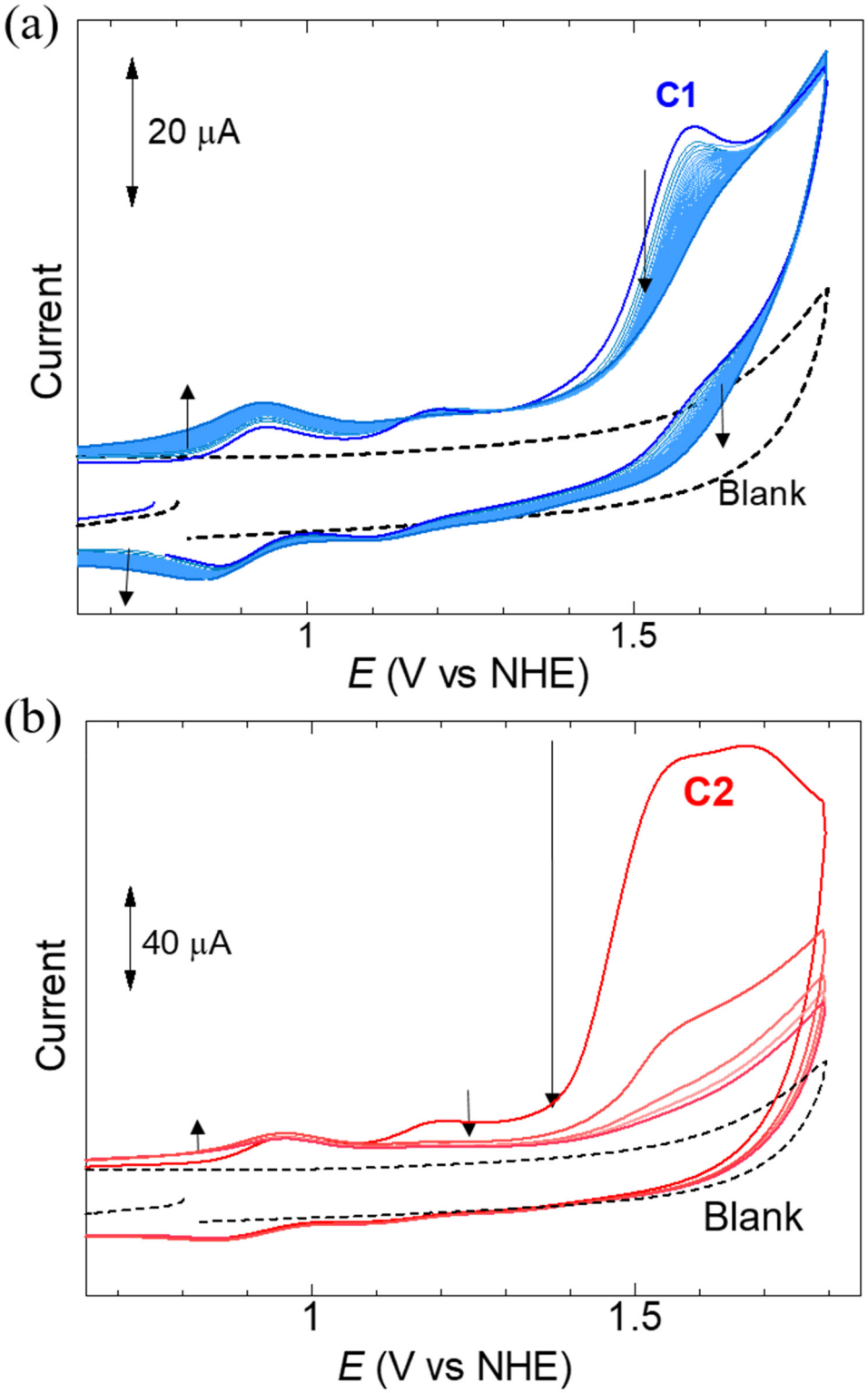

Figure S4. Changes of cyclic voltammograms during potential sweep cycles of (a) **C1** (1-50th cycles) and (b) **C2** (1-5th cycles). (200 μM, 0.1 M $NaClO_4$ solution of $HClO_4$ aq(pH=1.0)/TFE/acetonitrile (v/v/v=1/2/1) mixture).

Table S1. MO energies of each complex estimated by DFT calculation.

	C0 (eV)	**C1** (eV)	**C2** (eV)
LUMO+6			-0.9293
LUMO+5	-0.7301	-0.9178	-0.9301
LUMO+4	-1.2849	-1.3331	-1.4504
LUMO+3	-1.3396	-1.4468	-1.4803
LUMO+2	-1.5543	-1.5856	-1.6172
LUMO+1	-1.8071	-1.8381	-1.8653
LUMO	-2.3301	-2.3535	-2.3742
HOMO	-4.8747	-4.9008	-4.9247
HOMO-1	-5.2055	-5.2211	-5.2311
HOMO-2	-5.4483	-5.4426	-5.4347
HOMO-3	-6.1620	-5.8314	-5.8249
HOMO-4	-6.2350	-6.0760	-5.8630
HOMO-5	-6.6034	-6.1933	-6.0875
HOMO-6	-6.7389		-6.0875

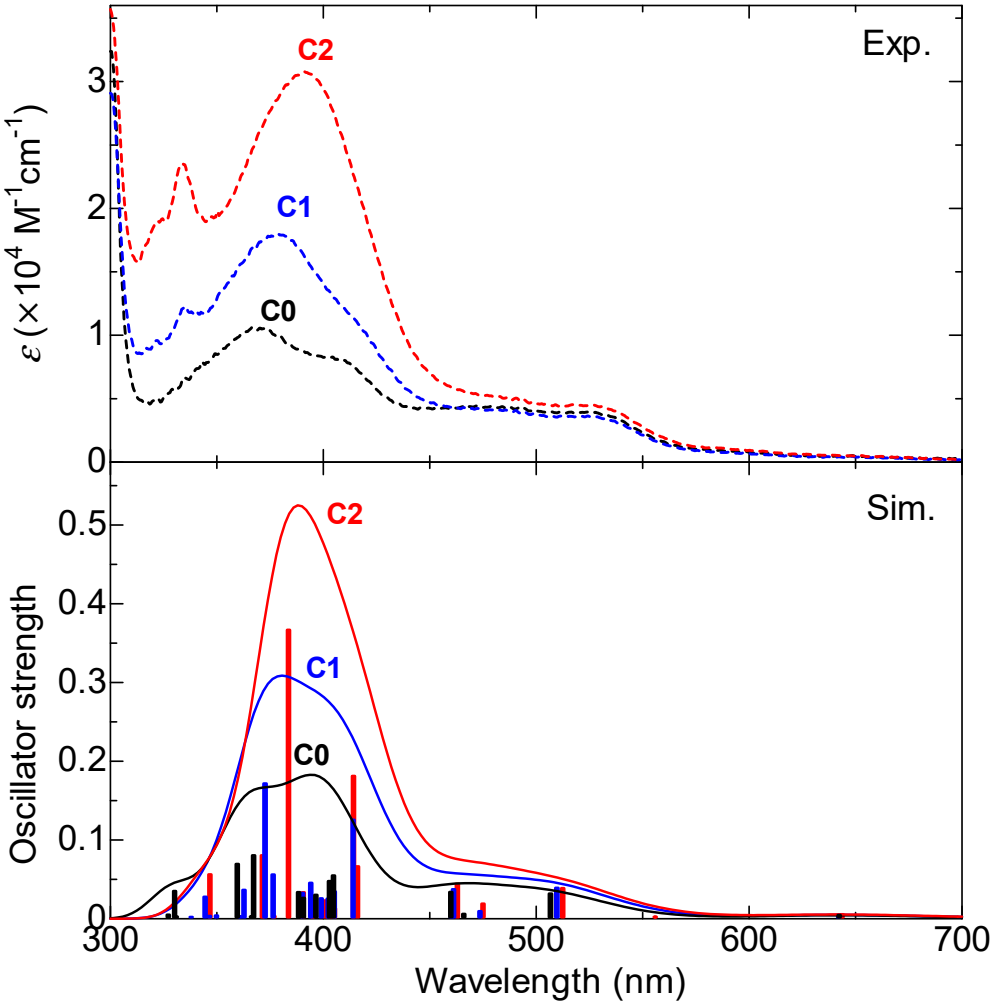

Figure S5. Comparison with (top) experimental spectra in dichloromethane/methanol (v/v=9/1) and (bottom) simulated absorption spectra by TD-DFT calculations of **C0** (black), **C1** (blue) and **C2** (red). The values of calculated oscillator strength are plotted as bar charts.

Table S2. Wavelength, oscillator strength (*f*), and contributions of major spin-allowed transitions (*f* > 0.01) of **C0**.

No.	λ (nm)	*f*	Contributions		(%)	Assignment
1	507.05	0.0316	HOMO-2	->LUMO	77	MLCT : Ru(d) -> bda(π*)
			HOMO-1	->LUMO+2	15	
2	460.21	0.0338	HOMO-1	->LUMO+1	93	MLCT : Ru(d) -> bda(π*)
3	405.18	0.0547	HOMO-2	->LUMO+1	7	MLCT : Ru(d) -> bda(π*) +py(π*)
			HOMO-1	->LUMO+2	55	
			HOMO-1	->LUMO+4	30	
4	403.22	0.0476	HOMO-2	->LUMO+2	14	MLCT : Ru(d) -> py(π*)
			HOMO-2	->LUMO+4	11	
			HOMO-1	->LUMO+3	60	
			HOMO	->LUMO+9	11	
5	396.85	0.0300	HOMO-2	->LUMO+2	47	MLCT : Ru(d) -> bda(π*)
			HOMO-1	->LUMO+3	27	
			HOMO	->LUMO+9	20	
6	390.99	0.0262	HOMO-2	->LUMO	7	MLCT : Ru(d) -> py(π*)
			HOMO-2	->LUMO+1	6	
			HOMO-2	->LUMO+3	48	
			HOMO-1	->LUMO+2	10	
			HOMO-1	->LUMO+4	20	
			HOMO	->LUMO+8	6	
7	388.7	0.0335	HOMO-2	->LUMO+2	29	MC : Ru(d) -> Ru(d)
			HOMO	->LUMO+9	60	
8	367.63	0.0802	HOMO-2	->LUMO+4	71	MLCT : Ru(d) -> py(π*)
			HOMO-1	->LUMO+3	8	
			HOMO	->LUMO+6	18	
9	359.95	0.0694	HOMO-2	->LUMO+4	14	MLCT : Ru(d) -> py(π*)
			HOMO	->LUMO+6	78	
10	330.48	0.0349	HOMO-6	->LUMO	85	LC : bda(π) -> bda(π*)
			HOMO-1	->LUMO+6	8	

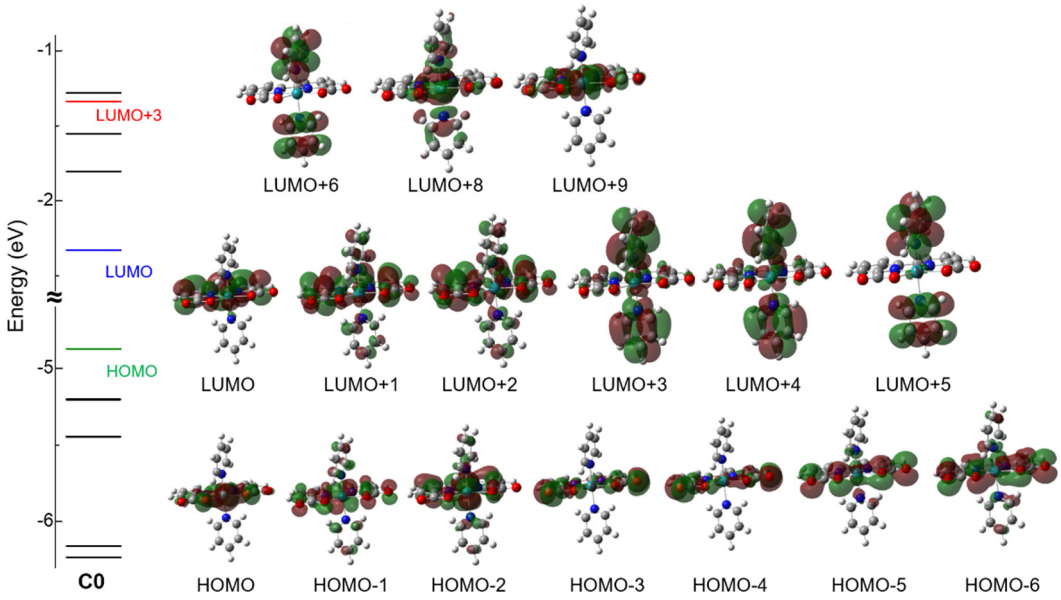

Figure S6. Schematic molecular orbital diagrams and orbital shapes of **C0** in the ground S_0 state.

Table S3. Wavelength, oscillator strength (*f*), and contributions of major spin-allowed transitions (*f* > 0.01) of **C1**.

No.	λ (nm)	*f*	Contributions [a]		(%)	Assignment
1	510.05	0.0390	HOMO-2	->LUMO	76	MLCT : Ru(d) -> bda(π*)
			HOMO-1	->LUMO+2	12	
2	461.48	0.0371	HOMO-1	->LUMO+1	93	MLCT : Ru(d) -> bda(π*)
3	414.35	0.1253	HOMO-1	->LUMO+2	45	MLCT :
			HOMO-1	->LUMO+3	38	Ru(d) -> bda(π*)+cbz-py(π*)
4	405.51	0.0342	HOMO-3	->LUMO	10	MLCT : Ru(d) -> cbz-py(π*)
			HOMO-2	->LUMO+3	10	
			HOMO-1	->LUMO+2	17	
			HOMO-1	->LUMO+3	21	
			HOMO-1	->LUMO+4	23	
5	402.61	0.0252	HOMO-3	->LUMO	48	LLCT : cbz-py(π) -> bda(π*)
			HOMO-2	->LUMO+2	10	
			HOMO-1	->LUMO+4	21	
6	399.34	0.0257	HOMO-3	->LUMO	9	MLCT : Ru(d)+ bda(π) -> bda(π*)
			HOMO-2	->LUMO+2	45	
			HOMO-1	->LUMO+3	8	
			HOMO-1	->LUMO+4	7	
			HOMO	->LUMO+11	23	
7	394.44	0.0453	HOMO-3	->LUMO	26	MLCT : Ru(d) -> cbz-py(π*)
			HOMO-2	->LUMO+3	33	
			HOMO-1	->LUMO+2	6	
			HOMO-1	->LUMO+4	16	
8	390.55	0.0323	HOMO-2	->LUMO+2	27	MC : Ru(d) -> Ru(d)
			HOMO	->LUMO+11	59	
9	376.75	0.0559	HOMO-2	->LUMO+3	15	MLCT : Ru(d) -> cbz-py(π*)
			HOMO-2	->LUMO+4	16	
			HOMO	->LUMO+6	58	
10	372.95	0.1714	HOMO-2	->LUMO+4	44	MLCT : Ru(d) -> py(π*)+cbz-py(π*)
			HOMO-1	->LUMO+3	6	
			HOMO	->LUMO+6	36	
11	363.07	0.0363	HOMO	->LUMO+7	90	MLCT : Ru(d) -> py(π*)

12	344.82	0.0275	HOMO-7	->LUMO	8	LLCT : cbz-py(π) -> bda(π*)
			HOMO-3	->LUMO+1	77	

[a]Minor contributions (< 5%) are omitted.

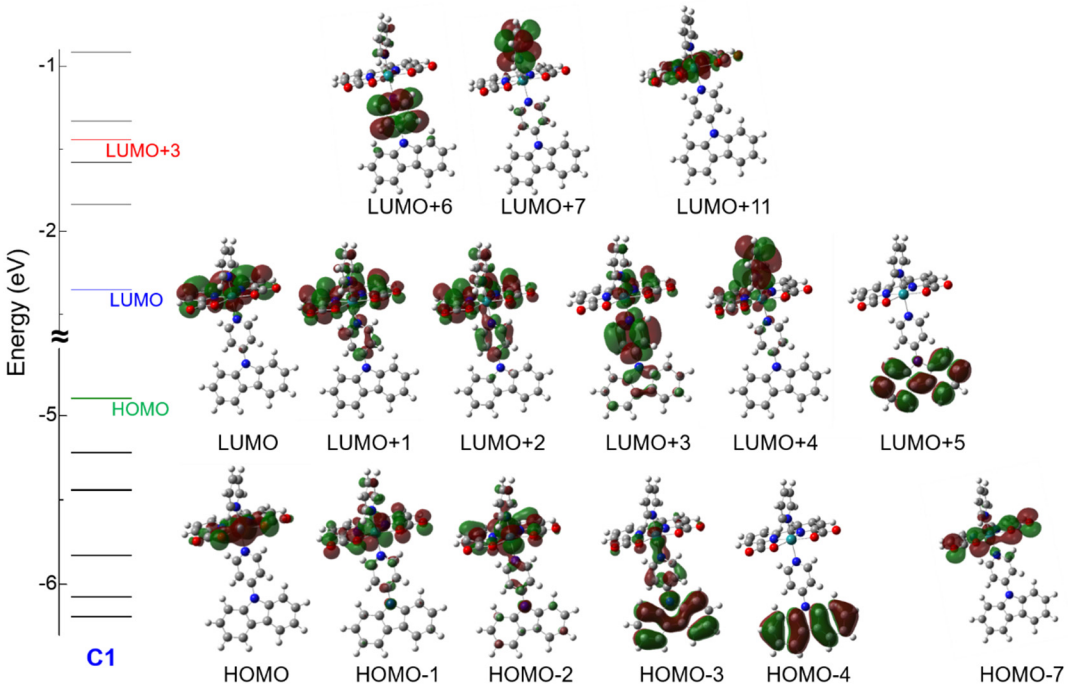

Figure S7. Schematic molecular orbital diagrams and orbital shapes of **C1** in the ground S_0 state.

Table S4. Wavelength, oscillator strength (*f*), and contributions of major spin-allowed transitions (*f* > 0.01) of **C2**.

No.	λ (nm)	*f*	Contributions [a]		(%)	Assignment
1	512.77	0.0385	HOMO-2	->LUMO	72	MLCT : Ru(d) -> bda(π*)
			HOMO-1	->LUMO+2	10	
			HOMO-1	->LUMO+4	7	
			HOMO	->LUMO+2	6	
2	475.38	0.0189	HOMO	->LUMO+3	94	MLCT : Ru(d) -> cbz-py(π*)
3	463.32	0.0441	HOMO-1	->LUMO+1	93	MLCT : Ru(d) -> cbz-py(π*)
4	416.39	0.0664	HOMO-2	->LUMO+1	6	MLCT : Ru(d) -> bda(π*)
			HOMO-1	->LUMO+2	68	
			HOMO-1	->LUMO+4	19	
5	414.49	0.1811	HOMO-2	->LUMO+4	8	MLCT : Ru(d) -> cbz-py(π*)
			HOMO-1	->LUMO+3	81	
6	405.54	0.0130	HOMO-4	->LUMO	34	LLCT : cbz-py(π) -> bda(π*) mixed with MLCT : Ru(d) -> cbz-py(π*)
			HOMO-2	->LUMO	10	
			HOMO-2	->LUMO+3	20	
			HOMO-1	->LUMO+4	22	
7	403.66	0.0125	HOMO-3	->LUMO	92	LLCT : cbz-py(π) -> bda(π*)
8	401.23	0.0229	HOMO-2	->LUMO+2	60	MLCT : Ru(d) -> bda(π*)
			HOMO-1	->LUMO+3	6	
			HOMO	->LUMO+13	20	
9	395.52	0.0236	HOMO-4	->LUMO	57	LLCT : cbz-py(π) -> bda(π*)
			HOMO-2	->LUMO+3	28	
10	390.88	0.0332	HOMO-2	->LUMO+2	19	MC : Ru(d) -> Ru(d)
			HOMO	->LUMO+13	65	
11	383.99	0.3667	HOMO-2	->LUMO+2	6	MLCT : Ru(d) -> cbz-py(π*)
			HOMO-2	->LUMO+4	82	
			HOMO-1	->LUMO+3	6	
12	371.75	0.0802	HOMO	->LUMO+8	96	MLCT : Ru(d) -> cbz-py(π*)
13	347.08	0.0560	HOMO-3	->LUMO+1	90	LLCT : cbz-py(π) -> bda(π*)

[a]Minor contributions (< 5%) are omitted.

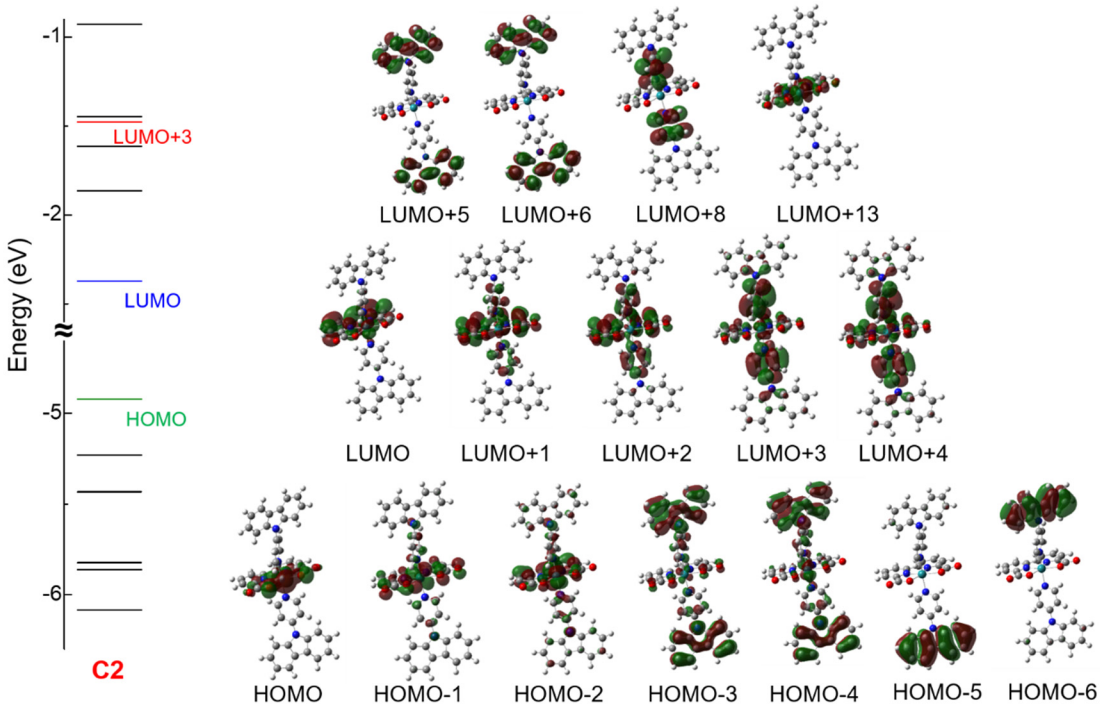

Figure S8. Schematic molecular orbital diagrams and orbital shapes of **C2** in the ground S_0 state.

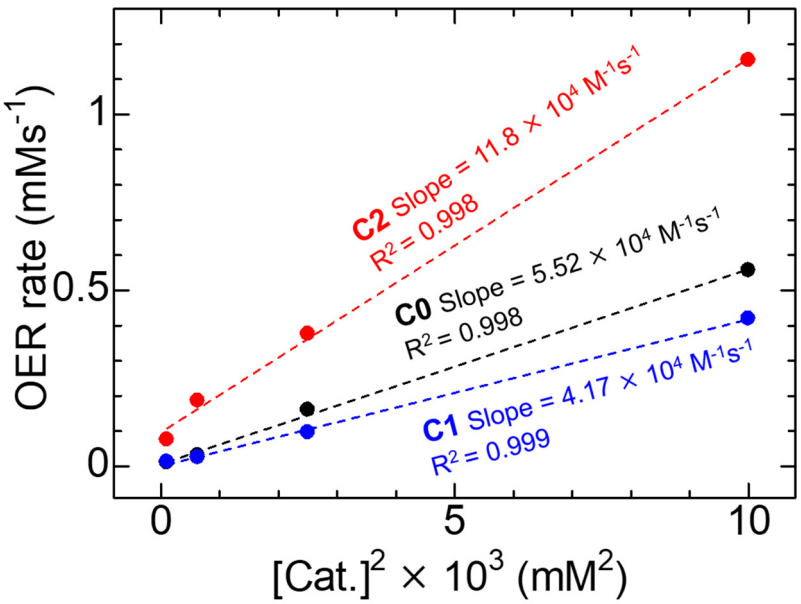

Figure S9. [Cat.] dependency of OER rate (= Evolved O_2 amount / Time) (Estimated from TOF_{max}).

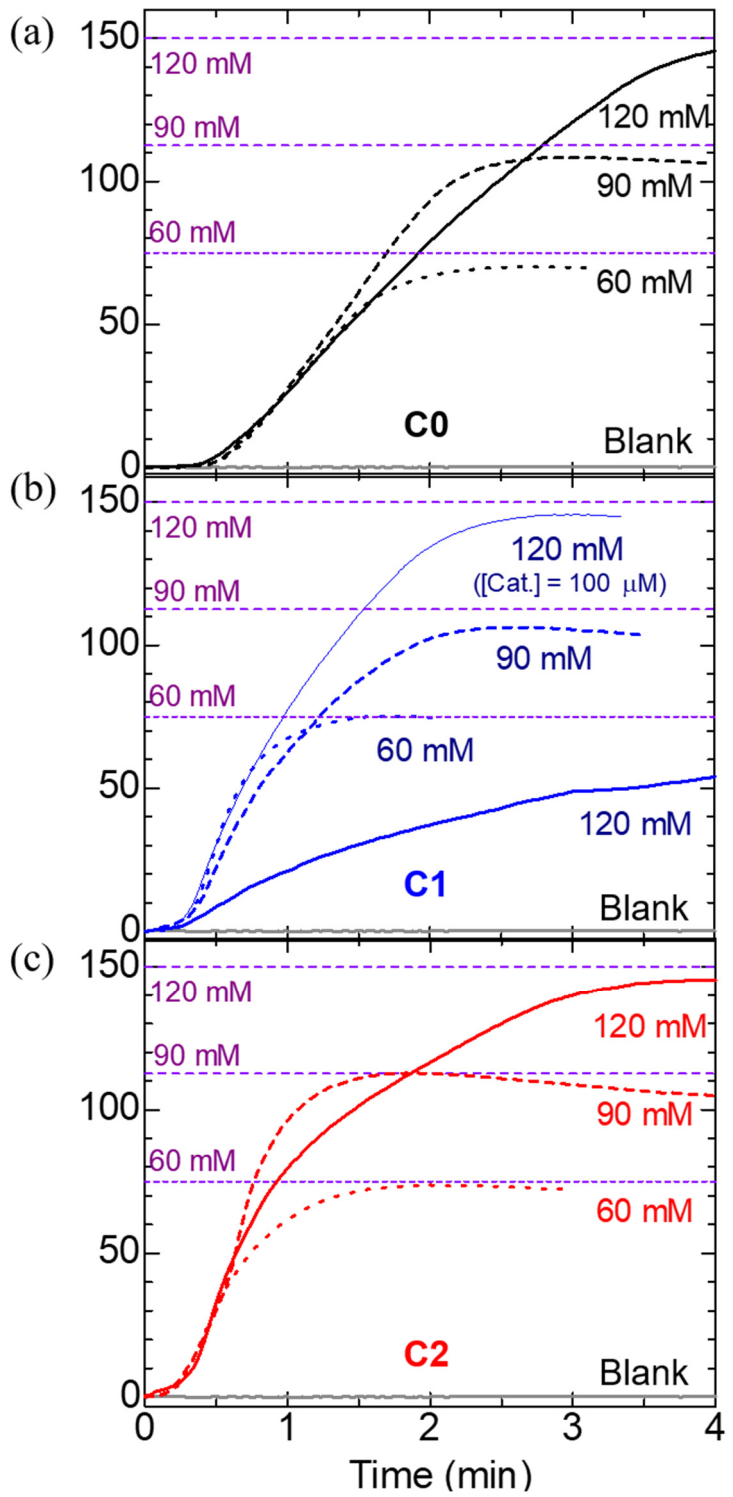

Figure S10. Chemical OER plots of (a) **C0** (b) **C1** (c) **C2**(50 μM) under [CAN] = 60-120 mM. [CAN] = 120 mM (bold lines), 90 mM (dashed lines) and 60 mM (dotted lines). Purple dashed lines in each panel show the calculated O_2 amounts based on the amount of one-electron oxidant CAN.

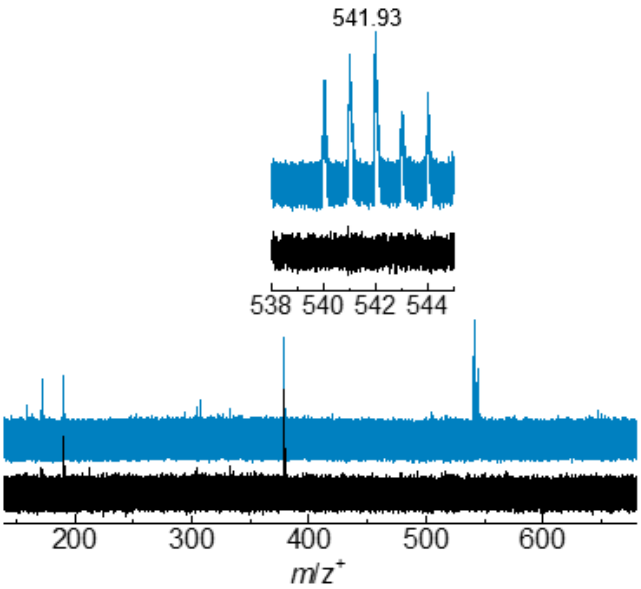

Figure S11. MALDI-MS spectra of the extract from the reaction mixture of **C1** ([**C1**] = 25 μM, [CAN] = 120 mM, in pH = 1.0 $HClO_4$ aq./TFE/acetonitrile (v/v/v = 3/2/1)) by CH_2Cl_2. The spectrum without the extract was shown as black solid line. The inset is the magnification of the peak assignable to a Ru-containing species. The exact structure of this species is unclear, but the mass is larger than that of $[Ru(bda)(py)_2]^+$ (m/z = 502), implying the coordination of cbz-py ligand to the Ru-bda unit. No significant peak at m/z ~ 250 assignable to the dissociated cbz-py species was observed.

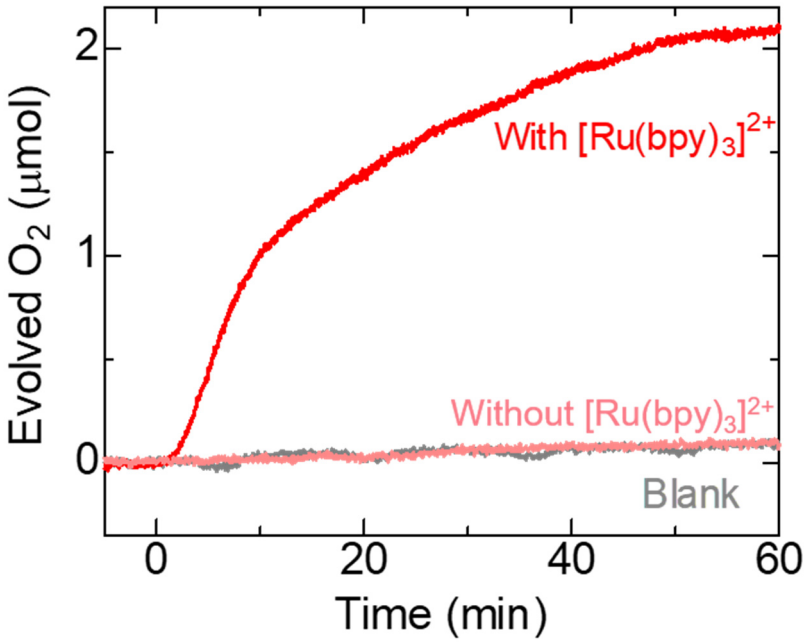

Figure S12. Photochemical OER plots of **C2** (10 μM) without $[Ru(bpy)_3]^{2+}$ in borate buffer (10 mM, pH = 8.0) aq./TFE /acetonitrile (v/v/v = 3/2/1). [Cat.] = 10 μM, $[Na_2S_2O_8]$ = 5 mM, λ = 470 nm, 30 $mWcm^{-2}$.

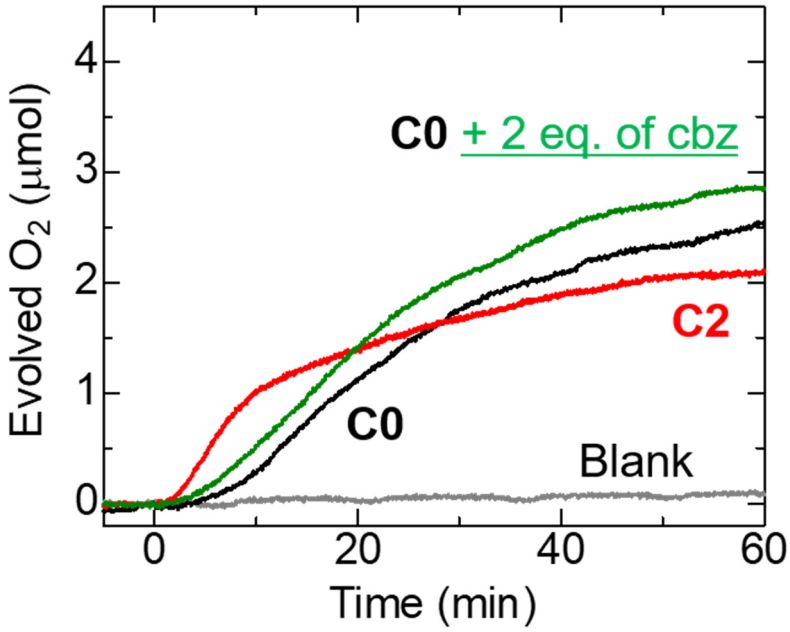

Figure S13. Photochemical OER plots of **C0** (10 μM) with cbz-H (20 μM) adduct.

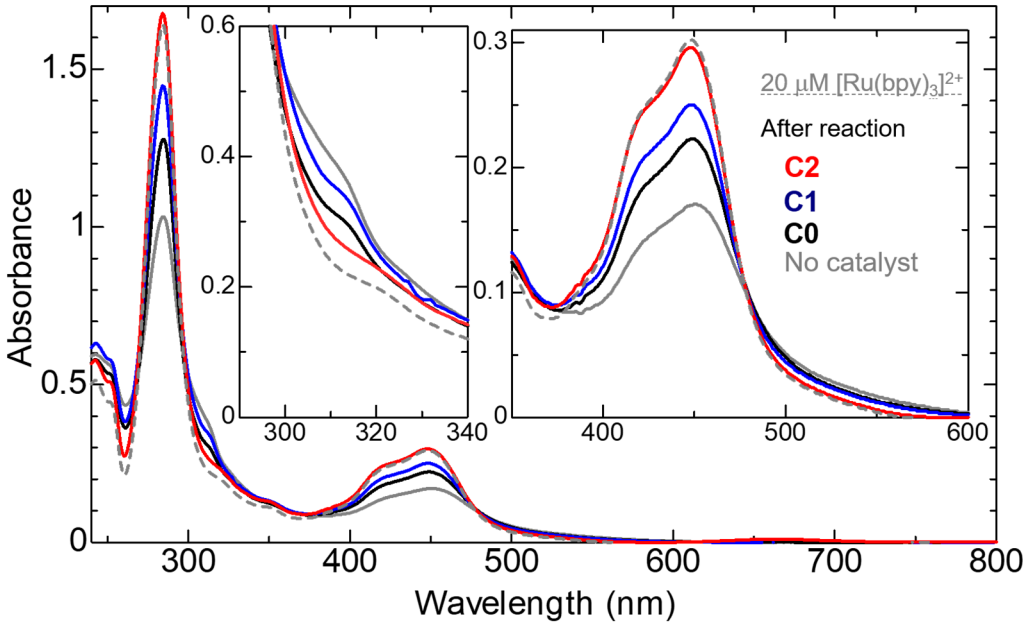

Figure S14. UV-Vis absorption spectra of reaction mixture after 1 h photolysis (solid line, red : **C2**, blue : **C1**, black : **C0** and no catalyst : gray. Diluted 10th fold.)and 20 μM$[Ru(bpy)_3]^{2+}$ soln. (gray, dashed line, pH=8.0, bubbled for 30 min and stated in the dark for 1 h).

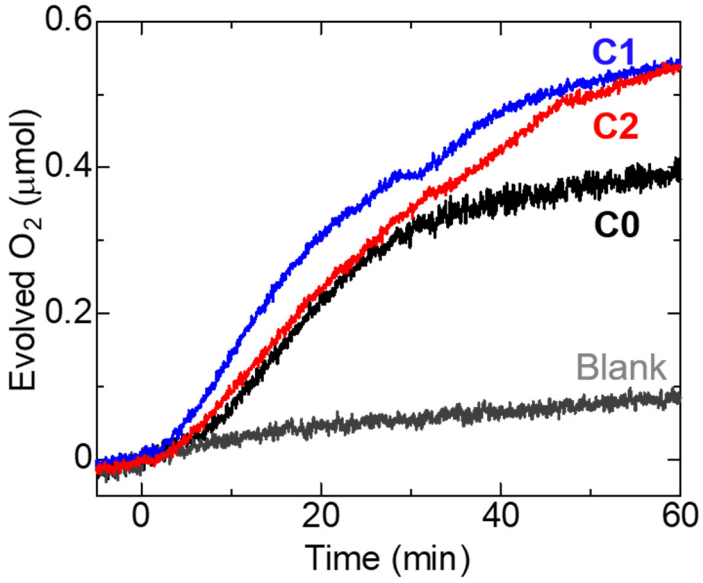

Figure S15. Photochemical OER plots of complexes **C0** (black), **C1** (blue) and **C2** (red) with Co^{III} oxidant in acetate buffer (40 mM, pH=5.0) aq. / TFE / acetonitrile (v/v/v = 3/2/1). [Cat.] = 10 μM, $[Ru(bpy)_3]^{2+}$ = 200 μM, ($[CoCl(NH_3)_5]^{2+}$ = 4 mM, λ = 470 nm, 30 $mWcm^{-2}$.

(a)

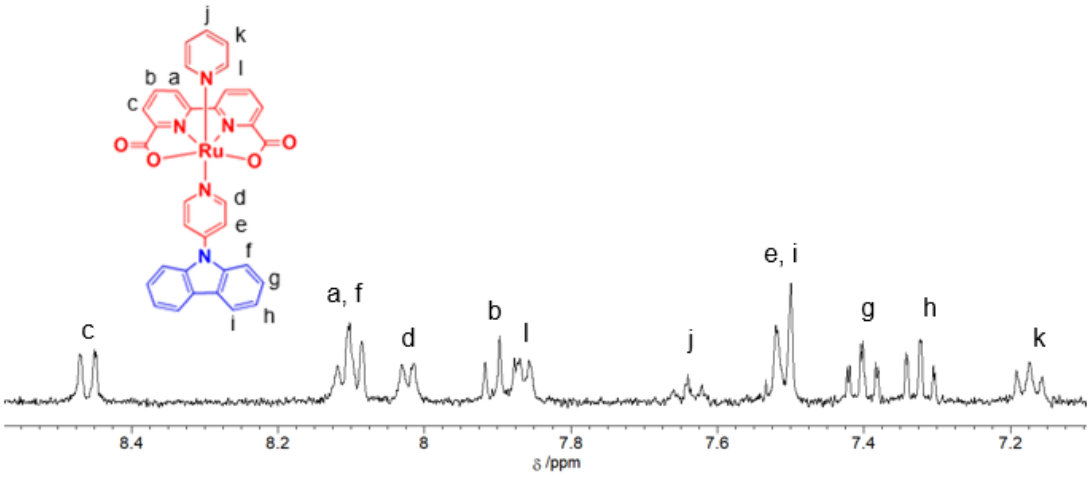

(b)

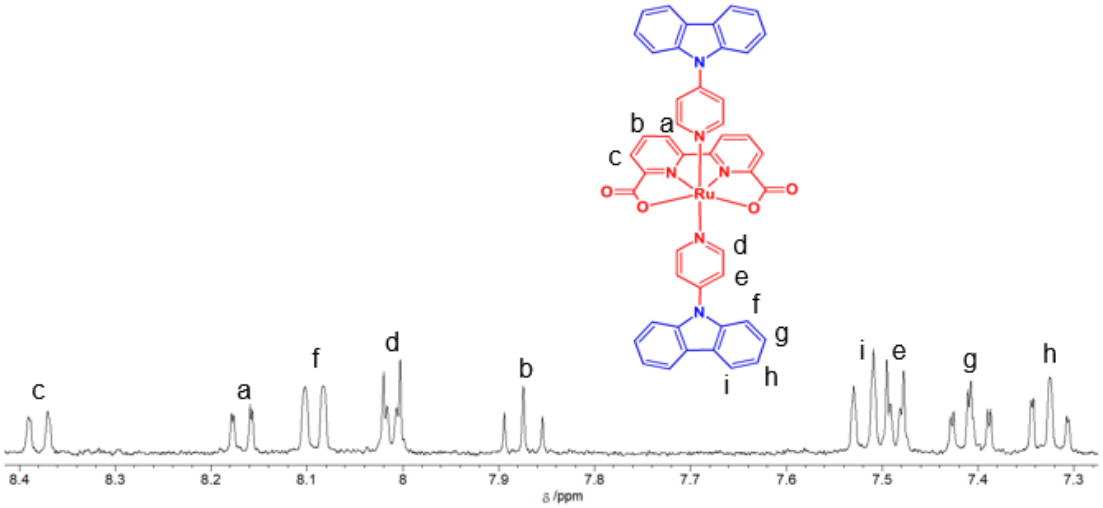

Figure S16. The aromatic region of ^{1}H NMR spectra of (a) **C1** and (b) **C2**. (400 MHz, CD_2Cl_2/methanol-d_4 with a small amount of L-ascorbic acid)

Table S5. Crystallographic parameters of. **C2**·$2CH_2Cl_2$.

Complex	**C2**·$2CH_2Cl_2$
T / K	150
Formula	$C_{46}H_{30}N_6O_4Ru \cdot 2CH_2Cl_2$
Formula weight	1001.68
Crystal system	*monoclinic*
Space group	$P2_1/n$
a / Å	8.08230(10)
b / Å	25.8123(5)
c / Å	20.3078(3)
α / deg.	90
β / deg.	93.8950(10)
γ / deg.	90
V / Å^3	4226.88(12)
Z	4
D_{cal} / g×cm^{-3}	1.574
Reflections collected	32223
Unique reflections	8639
GOF	1.100
R_{int}	0.0570
R (I > 2.00s(I))	0.0648
R_W [a]	0.1679

[a] $R_w = [\Sigma(w(F_o^2 - F_c^2)^2)/\Sigma w(F_o^2)^2]^{1/2}$.

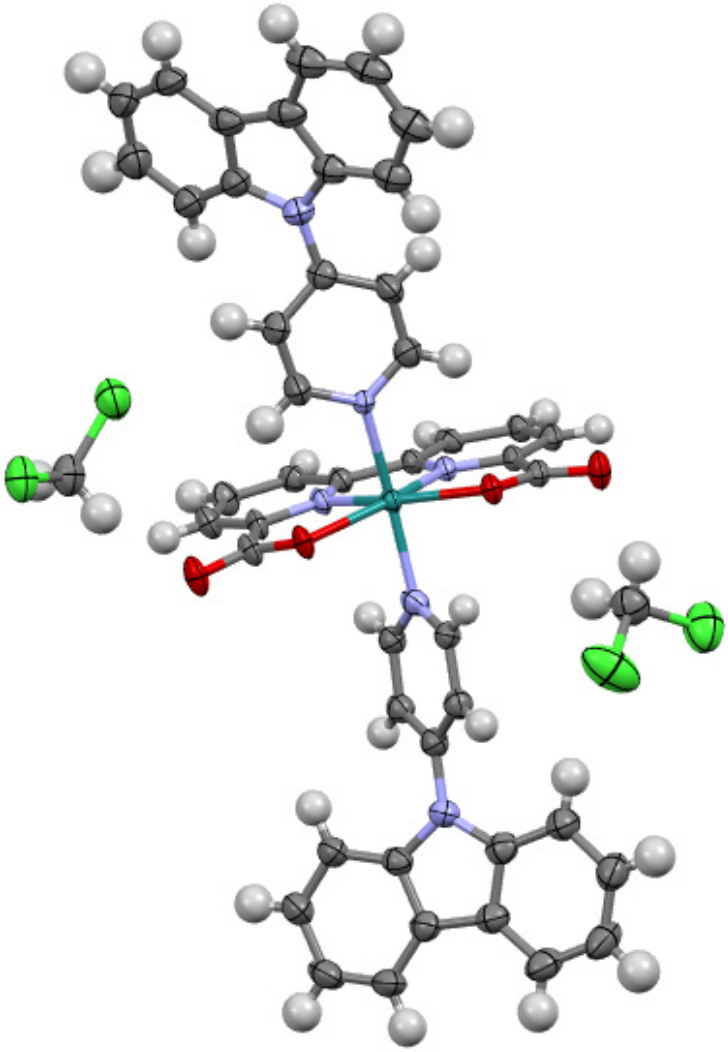

Figure S17. ORTEP drawings of. **C2**·2CH_2Cl_2. Thermal ellipsoids are shown at the 50% probability level. Color chart: grey: C, yellow green: Cl, white: H, purple: N, red: O, Green: Ru.